Catalysis Letters Vol. 91, Nos. 3–4, December 2003 (© 2003)

Photocatalytic water splitting over $La_2Ti_2O_7$ synthesized by the polymerizable complex method

Hyun Gyu Kim[a], Dong Won Hwang[a], Sang Won Bae[a], Jong Hyeon Jung[b], and Jae Sung Lee[a,*]

[a]*Department of Chemical Engineering/Institute of Environmental and Energy Technology,*
Pohang University of Science and Technology (POSTECH), San 31 Hyoja-dong, Pohang 790-784, Republic of Korea
[b]*Division of Biotechnology and Health Engineering, Sorabol College, Korea*

Received 14 August 2003; accepted 23 September 2003

Highly donor-doped (110) layered perovskite materials, $La_2Ti_2O_7$, with high surface areas were synthesized by the polymerizable complex (PC) method. Relative to $La_2Ti_2O_7$ prepared by the solid state reaction (SSR) method, PC catalysts showed higher surface areas, crystallization at lower temperatures, higher phase purity, more uniform morphology and better-distributed nickel on the outer surface of $La_2Ti_2O_7$. All these factors led to higher photocatalytic activity for overall water splitting under UV irradiation. The quantum yield of the reaction over $La_2Ti_2O_7$ prepared by the PC method was as high as 27%, which was about twofold greater than that over $La_2Ti_2O_7$ prepared by the SSR method.

KEY WORDS: $La_2Ti_2O_7$; polymerizable complex method; photocatalytic activity; water splitting.

1. Introduction

Perovskite-type oxide materials based on transition metals with d(0) electron configuration such as Nb (V), Ta (V) and Ti (IV) have been investigated as efficient photocatalysts for overall water splitting [1–7]. These photocatalysts have been prepared by the conventional solid-state reaction (SSR), in which appropriate amounts of precursor oxides or carbonates are ground together and then calcined at high temperatures (>1000 °C) for long hours to allow interdiffusion of cations. This preparation method produces materials of low surface areas, nonuniform particle sizes and low phase purity. These properties lead to a low photocatalytic activity. An improved synthesis method is in order that gives active photocatalysts with high surface areas [8]. The polymerizable complex (PC) method has been widely used to prepare multicomponent oxides at low temperatures. The method is based on condensation polymerization between ethylene glycol (EG) and citric acid (CA) in the presence of soluble metal–CA complexes. The complexes are immobilized in a rigid polyester network and allow formation of cationic species in the molecular level. Indeed, $K_2La_2Ti_3O_{10}$ prepared by the polymerized complex method was reported to have a high surface area due to the low-temperature heat treatment, and also to exhibit much higher activity than photocatalysts prepared by the conventional SSR method for photocatalytic water decomposition under ultraviolet (UV) irradiation [9,10].

Recently, we have succeeded in fabricating novel highly donor-doped (110) layered perovskite photocatalysts and discovered that the photocatalysts loaded with nickel show high quantum yields for overall water splitting under UV light [11–14]. These novel photocatalysts are a series of homologous structures with a generic composition of $A_mB_mO_{3m+2}$ ($m = 4, 5$; $A = \mathrm{Ca, Sr, La}$; $B = \mathrm{Nb, Ti}$). However, Brunauer–Emmett–Teller (BET) surface areas of these materials were very small ($\sim 1\,\mathrm{m^2/g}$) due to the high-temperature heat treatment needed to obtain crystalline phases. If the highly donor-doped (110) layered perovskite materials could be prepared using a low-temperature synthetic route, it might be possible to enhance the BET surface area of (110) layered perovskite materials, and thus to increase the photocatalytic activity for the water decomposition.

In this study, amorphous La_2O-TiO_2 powders were prepared by the polymerizable complex (PC) method, and crystalline $La_2Ti_2O_7$ powders were obtained by thermal treatment of the amorphous powders. The crystallization behavior of $La_2Ti_2O_7$ from the amorphous powders and their photocatalytic activity in water splitting were investigated and compared with the $La_2Ti_2O_7$ photocatalysts prepared by the solid-state reaction method.

2. Experimental

Figure 1 shows a flowchart of the synthesis procedure for $La_2Ti_2O_7$ crystals by the polymerizable complex method. Titanium isoproxide ($Ti(OCH(CH_3)_2)_4$, 99.0%, Aldrich), ethylene glycol ($C_2H_6O_2$, Kanto Chemicals), citric acid ($C_6H_8O_7$, Wako) and lanthanum nitrate

---

* To whom correspondence should be addressed.
E-mail: jlee@postech.ac.kr

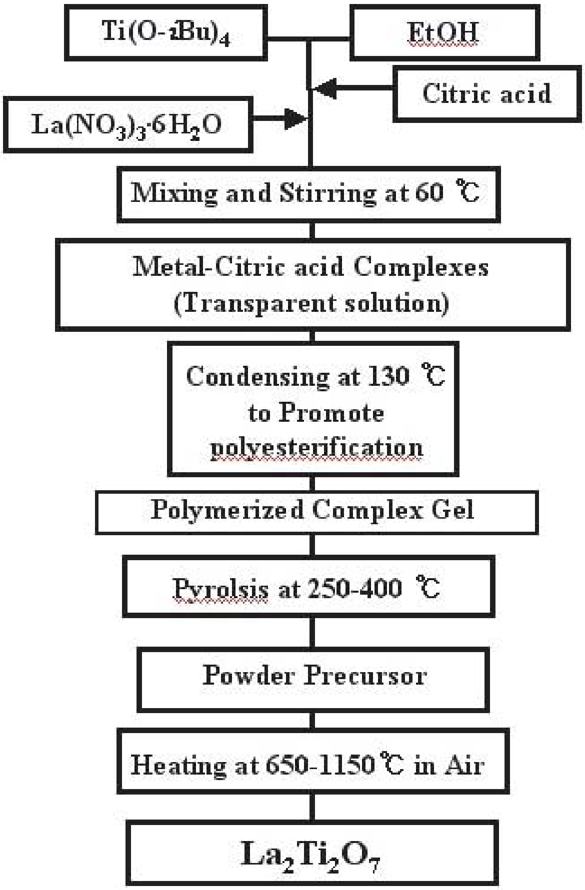

Figure 1. A flowchart for preparing $La_2Ti_2O_7$ by the polymerized complex method.

hydrate ($La(NO_3)_36H_2O$, 99.99%, Aldrich) were used as starting materials. After dissolving titanium isoproxide into ethylene glycol, an appropriate amount of anhydrous citric acid was added to convert $Ti(OCH(CH_3)_2)_4$ to stable Ti-citric acid complexes, and then a methanol solution containing La $(NO_3)_36H_2O$ was finally added. This solution was heated on a hot plate at 80 °C, until it became a transparent colorless solution. The solution was heated at 130 °C for several hours to obtain a polymeric gel. The viscous polymeric product was pyrolyzed at about 300–500 °C to form precursor powders. The powder precursor thus obtained was calcined at 500–1150 °C for 2 h to obtain crystalline $La_2Ti_2O_7$. For the purpose of comparison, $La_2Ti_2O_7$ was also prepared by the conventional solid-state reaction method. Crystalline $La_2Ti_2O_7$ powders were formed by heating a ground mixture of La_2O_3 (99%, Aldrich) and TiO_2 (99%, Aldrich) at 1150 °C for 24 h.

The $La_2Ti_2O_7$ crystals in the samples prepared by the polymerizable complex and the conventional solid-state reaction methods were characterized by X-ray diffraction (XRD, Mac Science Co., M18XHF) analysis. XRD peaks were compared with data from the Joint Committee Powder Diffraction Standards (JCPDS) for analysis. The band gap was measured by UV–vis diffuse reflectance spectroscopy (Shimadzu, UV 525). The BET surface area was evaluated by N_2 adsorption at the liquid nitrogen temperature in a constant volume adsorption apparatus (Micrometrics, ASAP2012) and the morphology was determined by scanning electron microscopy (SEM, Hitachi, S-2460N). Transmission electron microscopy (TEM, Philips, CM 200) was used to observe the dispersion of the metal on the oxide powders.

Photocatalytic reaction was carried out at room temperature in a closed gas-circulation system under UV generated from a high-pressure mercury lamp (Ace Glass Inc., 450 W) placed in an inner irradiation-type quartz reaction cell. The catalyst (0.3 g) was suspended in distilled water (500 mL) or aqueous solutions of additives by magnetic stirring. The rates of H_2 and O_2 evolution were determined from analysis of gas phase by gas chromatography (TCD, molecular sieve 5Å column and Ar carrier). The quantum yield of various photocatalysts was calculated by the chemical actinometer of potassium ferrioxalate $(K_3(Fe(C_2O_4)_3) \cdot 3H_2O)$ [15]. For the preparation of $K_3Fe(C_2O_4)_3 \cdot 3H_2O$, 1.5 M $K_2C_2O_4$ and 1.5 M $FeCl_3$ were mixed with stirring. The green precipitate was recrystallized three times in hot water and dried at −242 °C. For the measurement of photon flux, 500 mL of 0.006 M $K_3Fe(C_2O_4)_3 \cdot 3H_2O$ was illuminated for 60 s and then the absorbance at 510 nm of the mixture of the illuminated solution and 1,10-phenanthroline indicator was measured in a cell of 1 cm length.

3. Results and discussion

In order to examine crystallization behavior of $La_2Ti_2O_7$ in samples prepared by the PC method, their powder XRD patterns are shown in figure 2 in the 2θ range of 10–42°. The XRD patterns for the precursor and the samples treated below 650 °C were primarily those of amorphous solids, indicating that the precursor sample was not crystallized at low temperatures. The presence of both $La_2Ti_2O_7$ and amorphous phases in PC sample heat-treated at 700 °C was detected by XRD. A broad continuum around 25–35°, indicative of the presence of an amorphous phase, persisted even after raising the calcination temperature from 700 °C to 850 °C. However, all XRD reflections of the PC sample heat-treated above 900 °C exhibited a single phase of $La_2Ti_2O_7$. This result indicates that the crystallization of $La_2Ti_2O_7$ in PC sample is completed between 900 °C and 1100 °C.

Figure 3 compares the XRD patterns for a typical heat-treated PC sample (B) and an SSR sample (A). Both samples showed crystalline $La_2Ti_2O_7$ as the major phase. In the sample prepared by the SSR method at 1150 °C for 24 h, many impurity phases including La_2O and TiO_2 were observed. When the synthesis by the SSR method was done below 1150 °C, the impurity phases

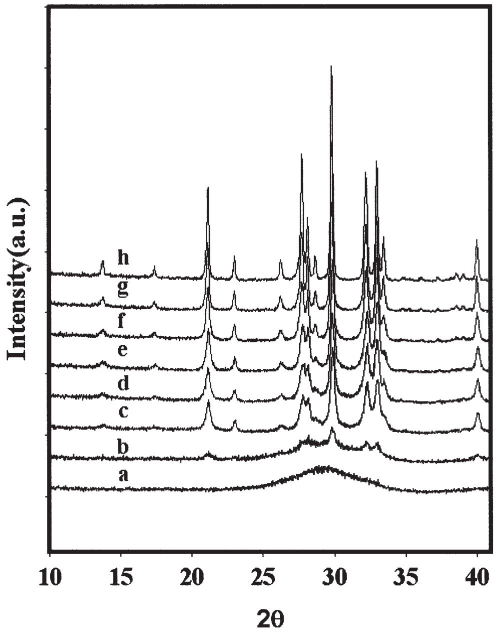

Figure 2. XRD patterns of (a) a precursor sample prepared by the PC method, and of $La_2Ti_2O_7$ formed from heat treatment at (b) 650 °C, (c) 700 °C, (d) 800 °C, (e) 900 °C, (f) 950 °C, (g) 1000 °C, (h) 1050 °C.

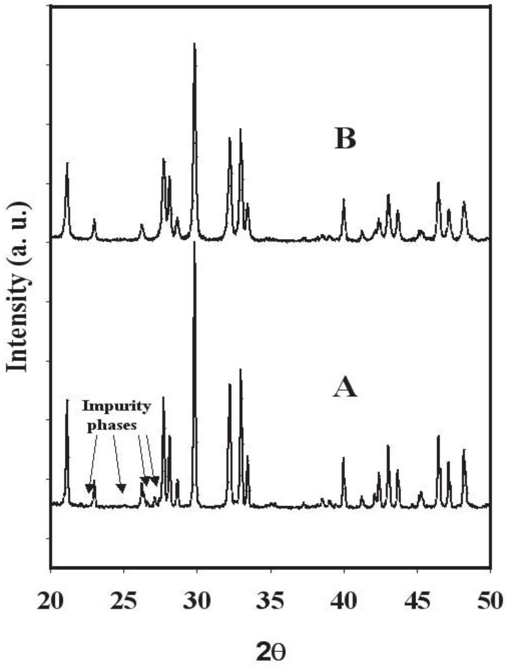

Figure 3. (A) XRD patterns at room temperature for the sample prepared by the SSR method at 1150 °C, and (B) the PC sample heat-treated at 1050 °C.

were found in higher concentrations. In the case of the PC sample (B) heat-treated at 1050 °C for 24 h, no impurity peaks were detected. Application of Scherrer's equation on the half width of XRD peaks (after correction for instrumental broadening) gave crystal sizes of 55.7 nm (SSR sample) and 55.4 nm (PC sample). Thus, the crystalline $La_2Ti_2O_7$ phase of the similar crystal size is formed at much lower temperatures by the PC method, and this indicates that crystallization of $La_2Ti_2O_7$ phase is much faster in PC samples. The lattice parameter of $La_2Ti_2O_7$ in figure 3 was estimated to be $a = 3.955$ Å, $b = 26.78$ Å and $c = 5.74$ Å (JCPDS-28-517). The crystal structure of $La_2Ti_2O_7$ is built up of layers of distorted perovskite-like slabs running parallel to the (110) plane bounded to each other by interlayer La^{3+} ions. The thickness of the slabs corresponds approximately to four corner-linked $(TiO_6)^{8-}$ octahedral.

Figure 4 shows SEM photographs for $La_2Ti_2O_7$ crystals prepared by PC method and SSR method. Both samples consist of fine particles that form agglomerates of 2–5 μm in size. These particles are agglomerates of crystals, 55.7 or 55.4 nm in average sizes as measured by XRD. Despite these similar crystal sizes, it is seen that the average particle size for $La_2Ti_2O_7$ formed in the heat-treated PC sample (figure 3(b)) is smaller and the morphology is relatively more uniform compared to those for the SSR sample (figure 3(a)).

Figure 5 shows UV–vis diffuse reflectance spectra for the heat-treated PC sample and the SSR sample. The wavelength at the absorption edge, λ_{ab}, was determined as the intercept on the wavelength axis for a tangent line as drawn in figure 5. Main absorption edges of both the heat-treated PC sample and the SSR sample were

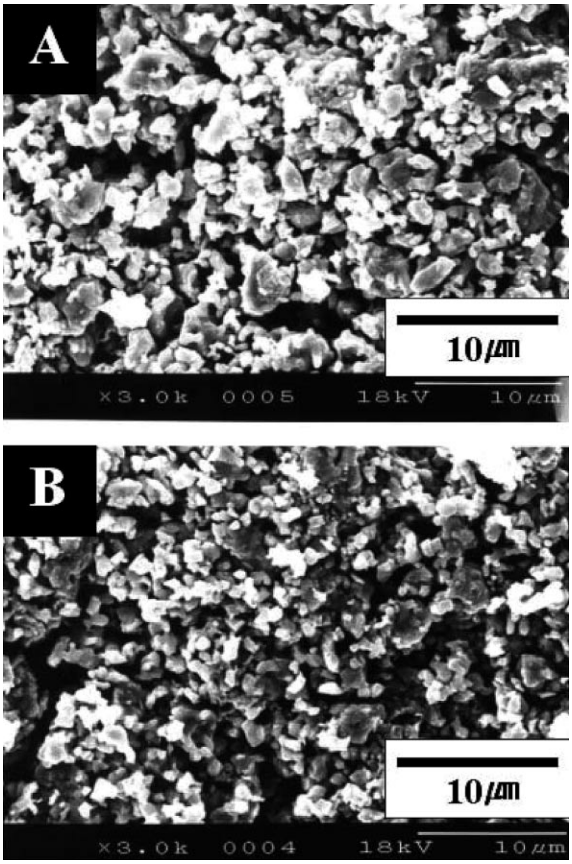

Figure 4. (A) The SEM photographs for the growth of $La_2Ti_2O_7$ crystal prepared by the SSR method at 1150 °C for 24 h, and (B) by the PC method at 1050 °C for 24 h.

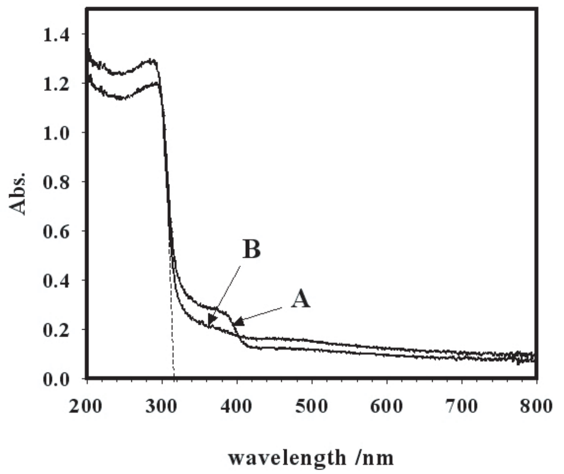

Figure 5. (A) The UV-DRS patterns of $La_2Ti_2O_7$ prepared by the SSR method at 1150 °C, and (B) by the PC method at 1050 °C.

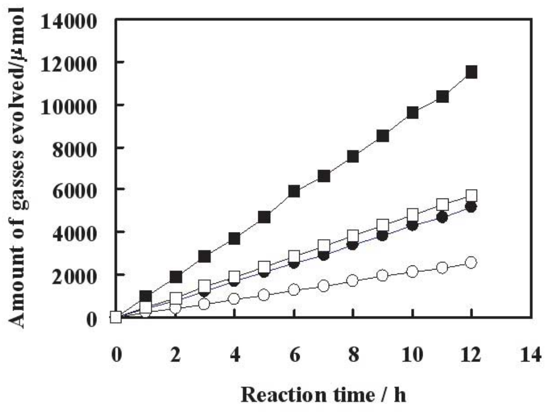

Figure 7. A typical time courses of H_2 and O_2 evolution over nickel-loaded PC sample (■: H_2, □: O_2) and nickel-loaded SSR sample (●: H_2, ○: O_2). Catalyst was pretreated by reduction at 700°C for 2 h followed by oxidation at 200 °C for 2 h. Reaction conditions: catalyst 1 g; distilled water 500 mL; light source: 450-W high-pressure mercury lamp placed in an inner irradiation reaction cell made of quartz.

estimated to be about 320 nm (3.87 eV). In addition, the SSR sample showed a shoulder peak at a wavelength of around 385 nm (3.2 eV), which was absent in the spectrum of the PC sample. This shoulder peak at 385 nm is probably due to the absorption by impurities. Otherwise, characteristics of the UV–vis spectra were the same for two samples.

The TEM images of nickel-loaded PC sample (A) and SSR sample (B) show nickel particles well dispersed on $La_2Ti_2O_7$ with average particle sizes of ca. 4 and 7 nm respectively, as shown in figure 6. Also, the nickel particles on the outer surface of PC sample (A) with the higher surface area showed a better distribution than that on the SSR sample. It is interesting to note the periodical fringes in figure 6(B) due to the layered structure of $La_2Ti_2O_7$. Their periodicity is 1.3 nm, which corresponds to slab thickness (10.54) plus an interlayer space (2.47) of $La_2Ti_2O_7$.

Activities of $La_2Ti_2O_7$ photocatalysts prepared by the PC method and heat-treated at various temperatures were compared with the $La_2Ti_2O_7$ prepared by the SSR method for photocatalytic water decomposition under UV irradiation, all under the same reaction conditions. Both the SSR samples and the heat-treated PC samples were loaded with nickel (0.1 wt%) and then pretreated by reduction at 500 °C for 2 h, followed by oxidation at 200 °C for 2 h. Figure 7 shows typical time courses of H_2 and O_2 gas evolution for the photocatalytic decomposition of water over a nickel-loaded PC sample (1050 °C) and SSR sample (1050 °C). Both samples produced H_2 and O_2 in a stoichiometric ratio ($H_2 : O_2 = 2 : 1$), indicating that

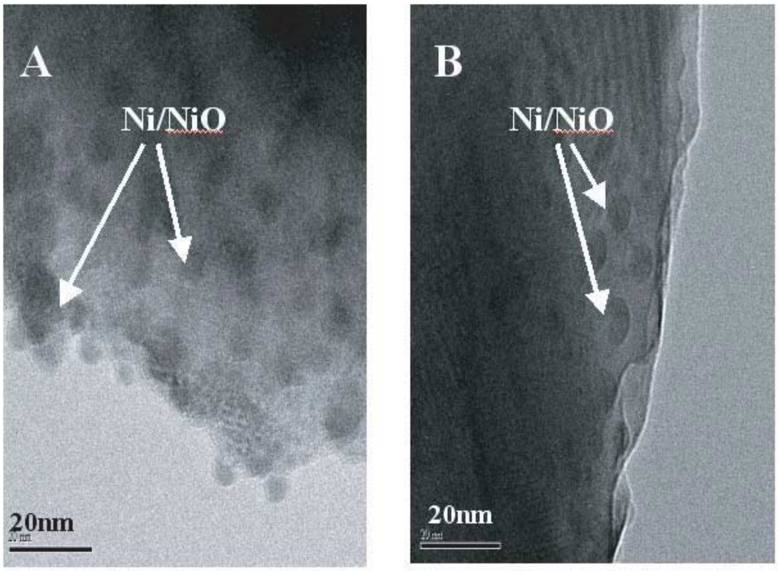

Figure 6. (A) The TEM images of Ni(1.0 wt%)/$La_2Ti_2O_7$. $La_2Ti_2O_7$ materials were prepared by PC method and (B) by SSR method Ni(0.1 wt%)/$La_2Ti_2O_7$ was pretreated by reduction at 700 °C for 2 h followed by oxidation at 200 °C K for 1 h.

Table 1
Photocatalytic activity of nickel-loaded $Li_2Ti_2O_7$ prepared by the PC method and the SSR method heat-treated at various temperatures

Catalysts	Calcination temperature (°C)	BET surface area ($m^2\,g^{-1}$)	H_2 evolution (μ mol/g_{cat}/h)	O_2 evolution (μ mol/g_{cat}/h)
PC sample (a)	650	20	–	–
PC sample (b)	700	20	–	–
PC sample (c)	750	20	–	–
PC sample (d)	800	19	2	–
PC sample (e)	850	17	7	3
PC sample (f)	900	12	11	4
PC sample (g)	950	8	18	6
PC sample (h)	1000	6	47	17
PC sample (i)	1050	5	960	478
PC sample (j)	1100	2	790	346
PC sample (k)	1150	1	442	218
SSR sample (l)	1000	2	340	167
SSR sample (m)	1050	2	387	190
SSR sample (n)	1100	1	408	197
SSR sample (o)	1150	1	440	217

Note: PC samples (a and b) were loaded with nickel (1.0 wt%) and then pretreated by the reduction at 500 °C for 2 h followed by oxidation at 200 °C for 1 h. PC samples (c–k) and SSR samples (l–o) were loaded with nickel (1.0 wt%) and then pretreated by the reduction at 700 °C for 2 h followed by oxidation at 200 °C for 2 h. The photocatalytic reaction was proceeded for 12 h under the following conditions: catalyst 1 g; distilled water 500 mL; light source: 450-W high-pressure mercury lamp placed in an inner irradiation reaction cell made of quartz.

overall water splitting was proceeding. The time course plots for both samples showed straight lines without any sign of deactivation during 12 h of the reaction.

Table 1 summarizes the results of water decomposition and BET surface areas for SSR and PC samples treated at different calcinations temperatures. The surface area of the precursor PC sample was $24\,m^2\,g^{-1}$, while that of $La_2Ti_2O_7$ prepared by SSR method was $1–2\,m^2\,g^{-1}$. Surface areas of $La_2Ti_2O_7$ prepared from the PC sample decreased with increasing heat-treatment temperatures as shown in the Table. At the same sintering temperatures, surface areas of PC samples were higher than those of the SSR sample except for the highest temperature (1100 °C) where two samples showed the same low surface area of $1\,m^2\,g^{-1}$.

The precursor PC sample consisting of the amorphous phase showed no activity for photocatalytic water decomposition. Photocatalytic activity of $La_2Ti_2O_7$ prepared by the PC method increased as the temperature of heat treatment was increased. Heat treatment at 1050 °C made a photocatalyst of the highest activity. It could be understood that the low activities of the PC samples (a–h) are closely related to the presence of the noncrystallized phase in the PC sample due to low heat-treatment temperatures. The activity showed a maximum for the catalyst (i) heat-treated at 1050 °C and then decreased upon heat treatment at higher temperatures (j and k). In the case of catalysts prepared by the SSR method, photocatalytic activity increased with increasing calcination temperature. However, the activities of SSR samples prepared at calcinations temperatures of 1050 °C and 1100 °C are much lower than those of the PC samples heat treated at the same temperatures. When two series samples with the same surface area (PC sample (j) and SSR samples (l) and (m)) are compared, the PC sample showed at least twofold higher activity than SSR samples. Thus, the low photocatalytic activities of SSR samples appear to be closely related to the presence of the impurity phases in these samples, as shown in figure 3, in addition to the effect of lower surface areas. At the severe heat-treatment condition (1150 °C), the surface area and the photocatalytic activity of both the PC and SSR samples were similar. The above results indicate that crystallization of $La_2Ti_2O_7$ in PC sample was one of the important factors in obtaining a high photocatalytic activity for photocatalytic water decomposition.

The quantum yields of water-splitting reaction were calculated for a PC sample and an SSR sample that showed the maximum activities among their series of samples. The quantum yield for H_2 evolution on the nickel-loaded $La_2Ti_2O_7$ photocatalyst prepared by the PC method and heat-treated at 1050 °C was ca. 27%. On the other hand, the quantum yield of the nickel-loaded $La_2Ti_2O_7$ photocatalyst prepared by the SSR method at 1150 °C was ca. 12%.

In the case of the samples prepared by the SSR method below 1100 °C, $La_2Ti_2O_7$ phase was formed, but there were impurity phases including unconverted precursor oxides due to low heat-treatment temperatures. Therefore, the solid-state reaction between fine particles of La_2O and TiO_2 requires heat treatment at a relatively high temperature (>1100 °C) to obtain a pure $La_2Ti_2O_7$ phase. However, PC synthesis provides mixing of elements at a molecular level. This reduces

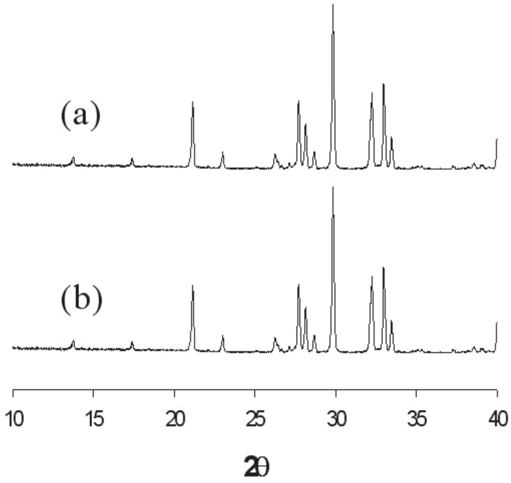

Figure 8. (a) XRD patterns of nickel (1.0 wt%)/$La_2Ti_2O_7$ before, and (b) after reaction. $La_2Ti_2O_7$ was prepared by the PC method and heat-treated at 1050 °C for 24 h. The nickel-loaded catalyst was pretreated by reduction at 700 °C for 2 h followed by oxidation at 200 °C for 1 h. The photocatalytic reaction was proceeded for 12 h under the following conditions: catalyst 1 g; distilled water 500 mL; light source: 450-W high-pressure mercury lamp placed in an inner irradiation reaction cell.

the length of diffusion path needed for obtaining the desired material down to the nanometer scale, and, as a consequence, needs a lower temperature to obtain the crystalline phase than the SSR method. Relative to the SSR method, the effects of low-calcination temperatures for the PC sample could be summarized as follows: [1] higher surface areas of $La_2Ti_2O_7$; [2] a higher phase purity of $La_2Ti_2O_7$; [3] more uniform morphology of $La_2Ti_2O_7$; [4] better-distributed nickel on the surface of $La_2Ti_2O_7$. Consequently, all these desirable properties of $La_2Ti_2O_7$ synthesized at relatively low temperatures (1050 °C–1100 °C) led to higher photocatalytic activities for overall water splitting under UV light irradiation.

In order to investigate the stability of the heat-treated PC sample under photocatalytic reaction conditions, we checked the structure of $La_2Ti_2O_7$ before and after photocatalytic reaction. The structure and crystalline state of $La_2Ti_2O_7$ before and after reaction were almost the same, as shown in figure 8. Thus, $La_2Ti_2O_7$ crystals prepared by the PC method are very stable under UV light and in the aqueous medium.

4. Conclusion

Highly donor-doped (110) layered perovskite materials, $La_2Ti_2O_7$, with high surface areas were fabricated by the PC method. The $La_2Ti_2O_7$ crystals in the sample prepared by the PC method were formed at a temperature lower than the temperature needed to obtain $La_2Ti_2O_7$ by the SSR method, but the structure and optical property of $La_2Ti_2O_7$ were almost the same. The desirable properties of $La_2Ti_2O_7$ prepared by the PC method appeared to be due to mixing of elements at a molecular level during the synthesis. The quantum yield of the heat-treated PC sample was much higher than that of the SSR sample for the photocatalytic decomposition of water under UV light. Photocatalytic activity of $La_2Ti_2O_7$ formed in the heat-treated PC sample depended on its crystallinity, surface area, phase purity and the dispersed state of nickel metal.

Acknowledgments

This work has been supported by KRF and BK-21 program of Korea Ministry of Education and Research Center for Energy Conversion and Storage through KOSEF and General Motors R&D Center.

References

[1] T.F. Wagner and A.G. Somorjai, J. Am. Chem. Soc. 102 (1980) 5494.
[2] S.M. Wrighton, B.A. Ellis and D.S. Ginley, J. Am. Chem. Soc. 98 (1976) 2774.
[3] K. Domen, A.N. Kudo and A. Shinozaki, Chem. Commun. (1986) 356.
[4] Y. Inoue, Y. Asai and K. Sato, J. Chem. Soc., Faraday Trans. 90 (1994) 797.
[5] A. Kudo and H. Kato, Chem. Lett. (1997) 867.
[6] T. Takata, Y. Furumi, K. Shinohara, A. Tanaka, M. Hara, J. Kondo and K. Domen, J. Photochem. Photobiol. A: Chem. 45 (1997) 106.
[7] K. Domen, M. Hara, J.N. Kondo, T. Takata, A. Kudo, H. Kobayashi and Y. Inoue, Korean J. Chem. Eng. 18(6) (2001) 862.
[8] M. Kakihana and M. Yoshimura, Bull Chem. Soc. Jpn. 72 (1999) 1427.
[9] S. Ikeda, M. Hara, J.N. Kondo and K. Domen, Chem. Mater. 10 (1998) 72.
[10] S. Ikeda, M. Hara, J.N. Kondo, K. Domen, H. Tkahashi, T. Okubo and M. Kakihana, J. Mater. Res. 13 (1998) 852.
[11] H.G. Kim, D.W. Hwang, J. Kim, Y.G. Kim and J.S. Lee, Chem. Commun. (1999)1077.
[12] D.W. Hwang, H.G. Kim, J. Kim, Y.G. Kim and J.S. Lee, J. Catal. 103 (2000) 40.
[13] J. Kim, D.W. Hwang, S.W. Bae, Y.G. Kim and J.S. Lee, Korean J. Chem. Eng. 18(6) (2001) 941.
[14] J. Kim, D.W. Hwang, H.G. Kim, S.W. Bae, Y.G. Kim, S.M. Ji and J.S. Lee, Chem. Commun. (2002) 2488.
[15] J.F. Rabek, *Experimental Methods in Photochemistry and Photophysics,* Part 2 (Wiley, New York, 1982).